

Accepted Article

1 Bottom mixing enhanced by tropical storm-generated 2 near-inertial waves entering critical layers in the Straits 3 of Florida

4 Lixin Qu¹, Leif Thomas¹, and Jonathan Gula^{2,3}

5 ¹Department of Earth System Science, Stanford University

6 ²Univ. Brest, CNRS, IRD, Ifremer, Laboratoire d'Oceanographie Physique et Spatiale, IUEM, Brest,
7 France

8 ³Institut Universitaire de France (IUF)

9 Key Points:

- 10 A slantwise critical layer for near-inertial waves is observed over the western slope
of the Straits of Florida.
- 11 • Signatures of near-inertial waves are observed in the slantwise critical layer after
tropical storms pass over the Straits of Florida.
- 12 • Upon entering the slantwise critical layer, the waves are trapped and hence am-
plified, leading to mixing enhancement over the western slope.

Corresponding author: Lixin Qu, lixinqu@stanford.edu

This article has been accepted for publication and undergone full peer review but has not been through
the copyediting, typesetting, pagination and proofreading process, which may lead to differences between
this version and the Version of Record. Please cite this article as doi: [10.1029/2021GL093773](https://doi.org/10.1029/2021GL093773).

This article is protected by copyright. All rights reserved.

Abstract

Tropical storms and hurricanes frequently pass over the Straits of Florida, energizing the near-inertial wave (NIW) field in the strait. Two ship-based surveys, which were launched shortly after storms, observed velocity shear bands over the western slope of the strait – clear signatures of NIWs. Also, the hydrographic measurements demonstrate the formation of a slantwise critical layer (where isopycnals are parallel with bathymetry) over the western slope, which is known to be a trapping zone for NIWs. A realistic simulation of the Straits confirms the emergence of NIWs under a tropical storm, which is accompanied by inertially-modulated bottom enhanced mixing over the western slope. The mechanism driving the mixing is that the storm-generated NIWs radiate downward from the core of the Florida Current, reflect off the eastern slope, and enter the slantwise critical layer over the western slope; upon entering, wave trapping and amplification lead to the enhanced mixing.

Plain Language Summary

Strong winds blowing over the ocean inject a significant amount of energy into the ocean. Some of this energy goes into near-inertial waves, internal waves radiating from the surface that transmit energy into the ocean interior. NIWs are thought to play a role in mixing deep waters and sustaining the global overturning circulation. However, they have not been considered as a key driver of mixing near the seafloor. In this study, we present observations of storm-generated NIWs over the seafloor of the Straits of Florida by two research cruises launched shortly after tropical storms. Supported by theories, our numerical simulations show supportive evidence that the seafloor mixing in the Straits of Florida can be enhanced by these storm-generated NIWs. The benthic deep-water coral ecosystems and the properties of intermediate water masses are potentially influenced by this mixing enhancement.

41 1 Introduction

42 Enhanced mixing over sloping bathymetry plays an important role in closing global
 43 ocean energy budgets and influences deep-water mass transformation and diapycnal up-
 44 welling, yielding significant implications for salinity, heat, and nutrient budgets in the
 45 abyssal ocean (Wunsch & Ferrari, 2004; Ferrari et al., 2016; McDougall & Ferrari, 2017;
 46 Callies & Ferrari, 2018). The bottom-enhanced mixing is highly localized, and one im-
 47 portant process driving it is critical reflection of internal waves (Kunze & Smith, 2004),
 48 which occurs when the wave's ray slope is close to the bottom slope. Under such circum-
 49 stances, the focusing of the wave energy would lead to wave amplification and hence wave
 50 breaking and enhanced mixing (Cacchione & Wunsch, 1974; Chalamalla et al., 2013).
 51 Observations over continental slopes have indicated that internal tides are the major agents
 52 undergoing critical reflection and inducing bottom-enhanced mixing as many continen-
 53 tal slopes are nearly critical for semidiurnal tidal periods (Moum et al., 2002; Nash et
 54 al., 2007; Gregg et al., 2012).

55 Near-inertial waves (NIWs) – inertia-gravity waves with a frequency near the in-
 56 erial frequency – carry a significant fraction of the kinetic energy in the internal wave
 57 field and are thought to contribute to ocean interior mixing. However, they have not re-
 58 ceived much attention in terms of critical reflection off sloping bathymetry (Alford et al.,
 59 2016). The lack of attention is mainly due to the conception that NIWs propagate nearly
 60 horizontally and that, when such waves encounter a steep slope, the waves would be re-
 61 reflected offshore rather than experiencing critical reflection (Cacchione et al., 2002; Kunze
 62 & Llewellyn Smith, 2004). However, theories suggest that the baroclinicity of an oceanic
 63 front can significantly steepen the propagation pathways of NIWs, opening the possibil-
 64 ity of the critical reflection of NIWs on sloping bottom (Mooers, 1975; Whitt & Thomas,
 65 2013; Thomas, 2017). Qu et al. (2021) demonstrate such a scenario – the so-called slant-
 66 wise critical layer which can form when isopycnals run parallel to sloping bathymetry.
 67 Upon entering this stratified layer, the wave's ray slope approaches the bottom slope with
 68 the alignment between the velocity shear bands and the sloping bathymetry, and, more
 69 importantly, the group velocity of the waves decreases to zero. Consequently, the wave
 70 amplification through trapping leads to turbulence and mixing in this stratified layer over
 71 the sloping bottom.

72 An example of a flow that satisfies the conditions for a slantwise critical layer is
 73 the benthic front that blankets the western slope of the Straits of Florida. A turbulent
 74 stratified boundary layer is observed within the benthic front with an averaged diffusiv-
 75 ity of $4.2 \times 10^{-4} \text{ m}^2/\text{s}$, which is one order of magnitude larger than the ambient water
 76 (Winkel et al., 2002). Using the scalings of Gregg (1989) and Polzin et al. (1995), Gregg
 77 et al. (1999) and Winkel et al. (2002) attributed the elevated mixing to turbulence as-
 78 sociated with the mean shear of the Florida Current and internal wave-wave interaction
 79 but they did not consider the trapping of NIWs in slantwise critical layers.

80 The Straits of Florida is heavily influenced by tropical storms, which input a sig-
 81 nificant amount of energy into the NIW field. In this article, we will demonstrate, us-
 82 ing a combination of numerical simulations and analyses of observations, that the trap-
 83 ping of storm-generated NIWs in slantwise critical layers can elevate mixing in the tur-
 84 bulent stratified boundary layer in the Straits.

85 2 Observations

86 A routine survey has been conducted at 27°N in the Straits of Florida to monitor
 87 the Florida Current transport since 2001 (Figure 1a) as part of the Western Boundary
 88 Time Series project (Meinen et al., 2010; Szuts & Meinen, 2013). The data collected dur-
 89 ing the surveys include hydrography from conductivity–temperature–depth (CTD) casts,
 90 and velocity measurements made using lowered acoustic Doppler current profilers (AD-

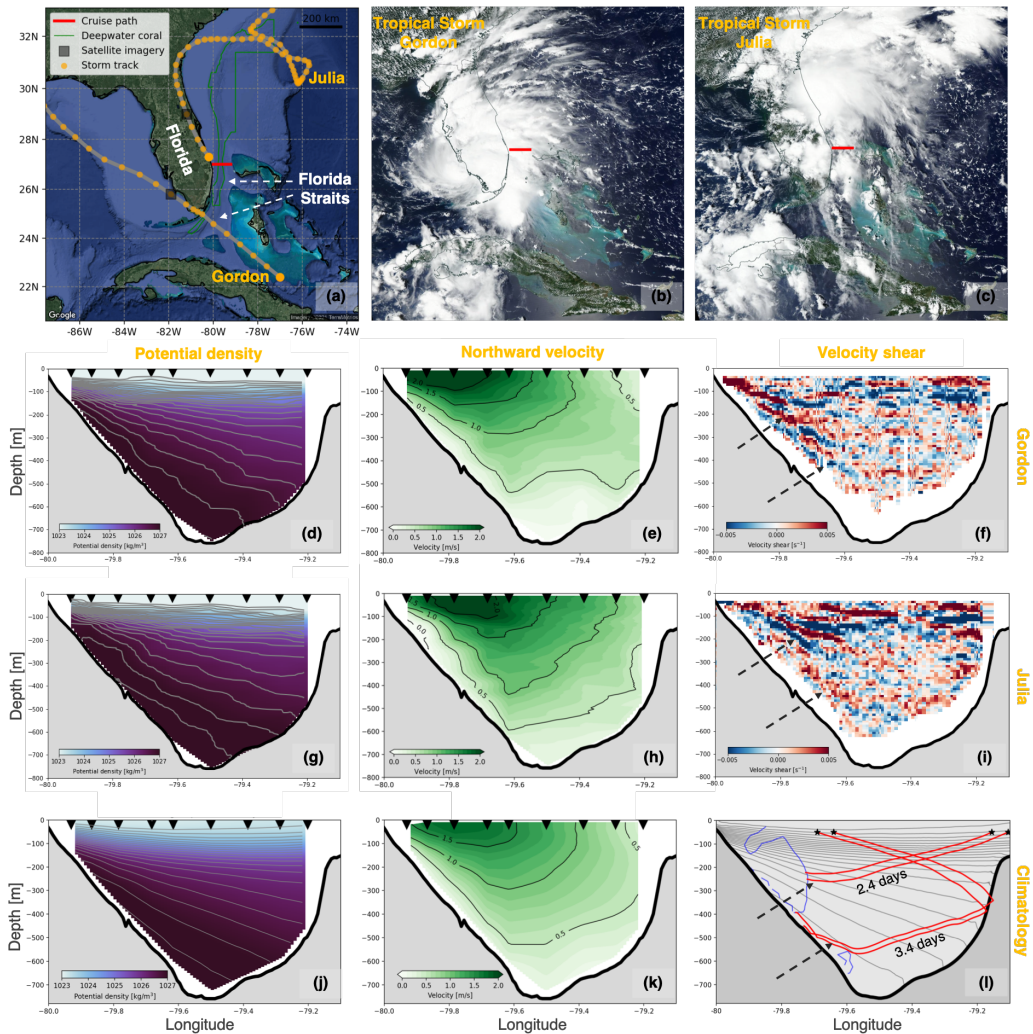


Figure 1. (a) Storm tracks and the cruise path in the Straits of Florida. The storm tracks are from the International Best Track Archive for Climate Stewardship (Knapp et al., 2010, IB-TrACS). (b and c) MODIS-AQUA visible images of Storms Gordon and Julia over the strait. The cruise path is marked by the red lines. (d-i) Potential density, meridional velocity, and vertical shear of zonal velocity from the cruises during Storms Gordon and Julia. The triangles denote the sampling stations. (j and k) Climatological averages of potential density and meridional velocity based on the cruises from 2001 to 2019. (l) Ray-tracing solutions. The black stars denote the initial locations of the waves, and the red rays are the pathways of the wave packets. The wave frequency is set to $1.1f|_{Lat=27^\circ N}$ (equivalent to a period of 24 hours). The blue contours mark the separatrix where $\omega_{min} = 1.1f$. The rays and the propagation time are estimated using the extrapolated field of the climatological potential density (contoured) and based on the ray-tracing theory (see the supporting information for details). Isopycnals in (d), (g), (j), and (l) are contoured in grey every 0.2 kg/m^3 .

CPs) and shipboard ADCPs (Garcia & Meinen, 2014). The CTD measurements were made at a resolution of 1 m at nine discrete stations (See Figure 1). During the CTD casts, the velocity measurements were made with a 300 kHz lowered ADCP at a resolution of 10 m. More continuous velocity fields across the strait were mapped at a resolution of 10 m in the vertical using a 75kHz shipboard ADCP which has a maximum profiling range up to 700 m. In this article, we use data collected by 75 cruises from 2001 to 2019, with 3-4 cruises per year.

Two out of the 75 cruises were conducted shortly (2-3 days) after large tropical storms passed the strait – one following Tropical Storm Gordon in September 2018, and the other following Tropical Storm Julia in September 2016 (Figure 1a, 1b, and 1c). Table S1 in the supporting information provides detailed information on the cruises and storms. These timely launches offer a unique opportunity for us to observe storm-generated NIWs. Both cruises observed the slantwise critical layer over the western slope of the strait, where the isopycnals run nearly parallel with the sloping bathymetry (Figure 1d and 1g). Moreover, tilted shear bands were observed over the western slope during both cruises, suggestive of the presence of NIWs (Figure 1f and 1i). The shear bands can be classified into two groups representing two different pathways of NIWs, with one group located at shallower depths (above ~ 200 m) and the other at deeper depths (below ~ 300 m). The deeper group of NIWs enter the slantwise critical layer, and the subsequent trapping and amplification of the NIWs should elevate mixing over the western slope according to the theory in Qu et al. (2021).

To identify the pathways of the two groups of NIWs, ray-tracing is conducted based on the climatology fields in the strait (see the supporting information for the theory behind the ray-tracing calculation). The climatology includes the potential density and meridional velocity, which are calculated based on the 19-years of cruise data. The climatological potential density suggests that the slantwise critical layer over the western slope is a persistent feature (Figure 1j). The climatological meridional velocity indicates that the vorticity at the surface changes sign in the core of the Florida Current (Figure 1k), where the vorticity gradient is likely maximum and hence a location for the downward radiation of NIWs (see Section 4.1). Another radiation location is at the eastern edge of the strait, where the vorticity gradient is also large (see Figure S1 in the supporting information). Wave rays are initiated at these locations and traced until they reach the separatrix, beyond which the waves become evanescent. As illustrated in Figure 1, we envision that the shallower NIWs originate from the eastern side of the strait, while the deeper NIWs radiate from the Florida Current, reflect off the eastern slope, enter the slantwise critical layer, and enhance mixing over the western slope.

3 Realistic simulation

Unfortunately, the surveys did not make fine-scale measurements of turbulence, and hence accurate mixing information can not be directly acquired. Moreover, information on temporal variations was not provided since each survey samples the whole strait only once each time. In lieu of such observations, we use a realistic simulation that is capable of reproducing the responses of the NIWs and associated mixing enhancement under tropical storms to explore the physics of NIWs in the Strait.

The realistic simulation is extracted from a submesoscale-permitting Atlantic wide simulation (GIGATL1) performed with the Coastal and Regional Ocean CCommunity model (CROCO), which is built upon the Regional Oceanic Modeling System (Shchepetkin & McWilliams, 2005, ROMS). It solves the free surface, hydrostatic, and primitive equations using terrain-following vertical coordinates. The simulation domain covers the full Atlantic Ocean with a horizontal resolution that varies between 700 m and 1 km and with 100 vertical levels. The simulation is run from June 2007 to June 2009. Boundary conditions are supplied by the Simple Ocean Data Assimilation (Carton & Giese, 2008, SODA).

Accepted Article

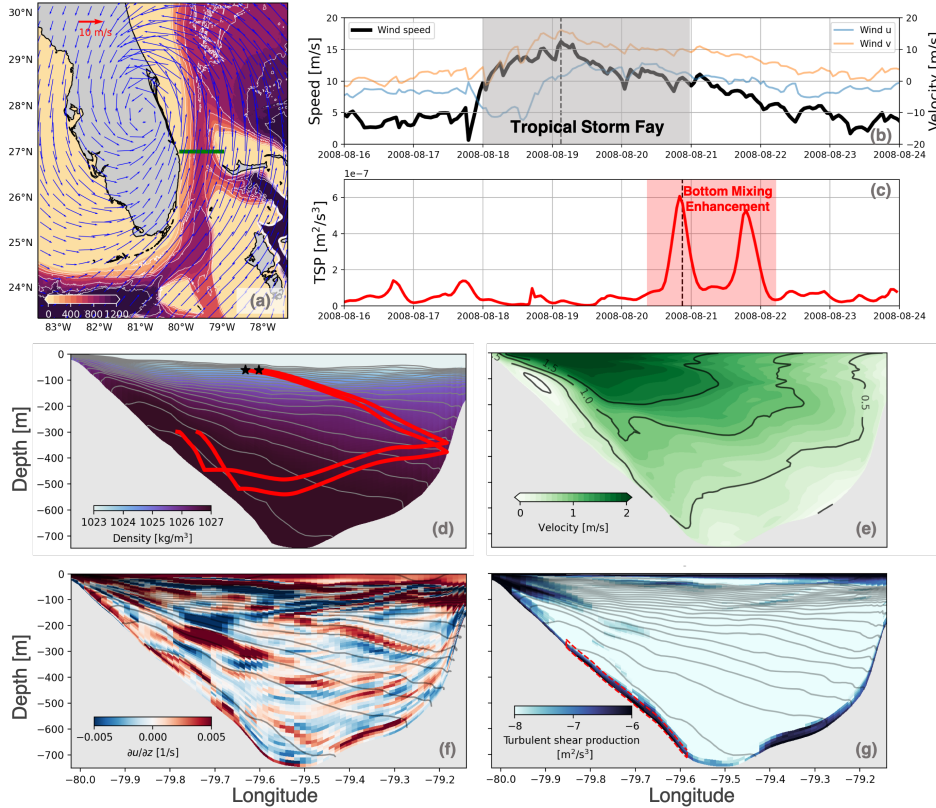


Figure 2. Results of the realistic simulation. (a) Surface winds (vectors) of Tropical Storm Fay from CFSR/NOAA and the strait bathymetry (color) from SRTM30plus. The snapshot of the winds is made at 03:00 on 08/19/2008, which is denoted in (b) by the dashed line. (b) Time series of the zonal (blue), meridional (yellow) components, and speed of the winds during the storm. The properties are averaged across the strait along 27 °N (along the green line in (a)). (c) Time series of the turbulent shear production, $P \equiv -\bar{u}'w^T \frac{\partial u}{\partial z} - \bar{v}'w^T \frac{\partial v}{\partial z} = \nu[(\frac{\partial u}{\partial z})^2 + (\frac{\partial v}{\partial z})^2]$, where ν is the viscosity. P is averaged within the control volume denoted in (g) by the dashed box. (d-g) Across-strait sections of the potential density, meridional velocity, vertical shear of zonal velocity, and turbulent shear production along 27 °N. The red lines in (d) are the wave rays calculated by setting the wave frequency of $1.1f|_{Lat=27^\circ N}$ (equivalent to a period of 24 hours). These sections are made at 21:00 on 08/20/2008, which is denoted in (c) by the dashed line. The potential density is contoured every 0.2 kg/m³ in (d), (f), and (g).

Initial conditions are provided by a lower resolution version ($dx = 3$ km) of an otherwise identical configuration initialized in January 2004 using SODA as initial and boundary conditions. The simulation is forced by hourly atmospheric forcings from the Climate Forecast System Reanalysis (Saha et al., 2010, CFSR) and includes barotropic tidal forcing at the boundaries and tidal potential and self attraction that are taken respectively from TPXO7.2 and GOT99.2b. The bathymetry is taken from the SRTM30plus dataset (Becker et al., 2009). The $k - \epsilon$ turbulence closure scheme is used to parameterize vertical mixing, and the Canuto A stability function formulation is applied (Umlauf & Burchard, 2003; Canuto et al., 2001). There is no explicit lateral diffusivity in the simulation. The effect of bottom friction is parameterized through a logarithmic law of the wall with a roughness length $Z_0 = 0.01$ m.

Here, we present the responses of the NIWs and associated mixing enhancement during Tropical Storm Fay, which moved over the strait in mid-August, 2008 (Figure 2a). At $27^\circ N$, the winds start to increase at 19:00 on August 17th and maintain a speed exceeding 10 m/s for about 3 days (Figure 2b). Noticing that the inertial period at $27^\circ N$ is 26.4 hours, the turbulent shear production $P \equiv -u'w' \frac{\partial u}{\partial z} - v'w' \frac{\partial v}{\partial z}$ over the western slope exhibits a near-inertial pulsing about 3 days after the wind burst (Figure 2c). The enhancement of P indicates the enhancement of mixing, because P is the direct energy supply for the turbulent kinetic energy (TKE) dissipation rate ϵ and the turbulent buoyancy flux $B \equiv -b'w'$ based on the $k - \epsilon$ model (Warner et al., 2005). The near-inertial variability of P suggests that the enhanced mixing is related to NIWs. As illustrated in Figure 2d, a slantwise critical layer is formed over the western slope, and the ray tracing solution suggests that the NIWs radiating from the Florida Current could enter the slantwise critical layer. This pathway of NIWs is indeed reflected in the field of vertical shear with the shear bands largely paralleling the wave rays (Figure 2f). Correspondingly, the mixing enhancement blankets the deep western strait (from 300 m to 700 m roughly) over a thickness of about 30 m. This region with the enhanced mixing coincides with the turbulent stratified boundary layers, that were identified by Winkel et al. (2002) using microstructure measurements at $27^\circ N$ in the strait. We explore the underlying mechanism driving the enhanced mixing within the stratified boundary layers over the western slope in the next section. The mixing over the eastern slope of the Straits is also near-inertially enhanced during the storm due to critical reflection of NIWs (see the supporting information for the detail).

4 Mechanism driving the mixing enhancement

4.1 Conceptual model

A simple 2D conceptual model is developed to illustrate the mechanism driving the mixing enhancement over the western slope of the strait (see the schematic in Figure 3). The model consists of three key elements: (1) radiation of NIWs out of the core of the Florida Current; (2) downward reflection of NIWs off the eastern slope; (3) trapping of NIWs in the slantwise critical layer over the western slope. Each element is elaborated in more detail below.

The storm inputs energy into near-inertial motions and energizes a NIW field with large horizontal scales near the surface. However, to radiate downwards, NIWs need to reduce their wavelength to increase their vertical group velocity. Via a mechanism known as ζ -refraction, the lateral wavelength of NIWs can be efficiently reduced at locations where gradients in vertical vorticity, ζ , are large, and, as the wavelength shrinks, the NIWs can radiate into the interior (Young & Jelloul, 1997; Asselin & Young, 2020). Based on the surface velocity profile (Figure S1 in the supporting information), the core of the Florida Current would be such a location where NIWs are preferentially radiated downwards via ζ -refraction.

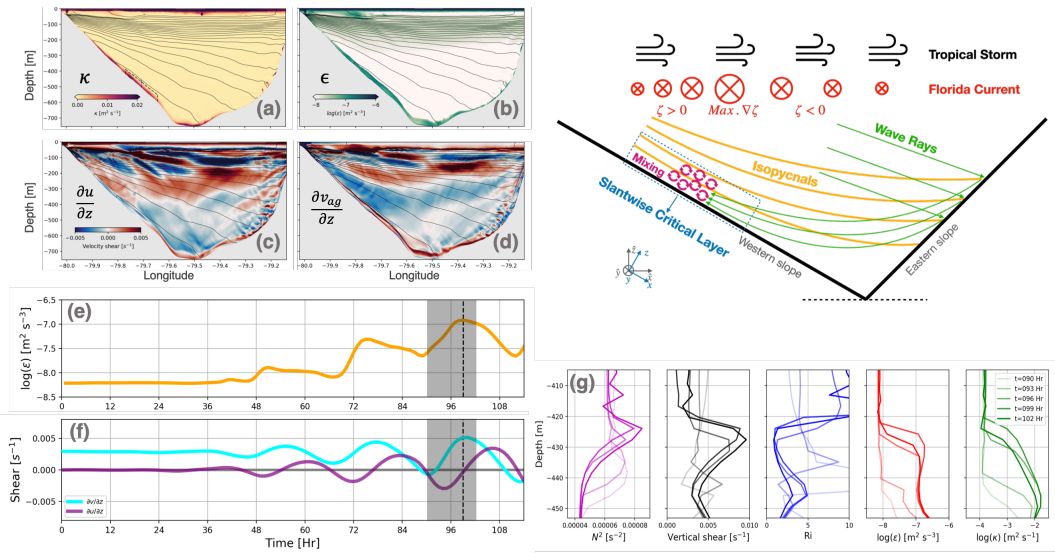


Figure 3. Schematic of the theoretical model and the idealized simulation results. (a-d) Across-strait sections of diffusivity κ , TKE dissipation rate ϵ , vertical shear of zonal velocity $\frac{\partial u}{\partial z}$, and vertical shear of ageostrophic meridional velocity $\frac{\partial v_{ag}}{\partial z}$. The sections are made at $t = 99\text{Hr}$ denoted by the dashed line in (e) and (f). The potential density is contoured very 0.2 kg/m^3 . (e and f) Time series of ϵ , $\frac{\partial u}{\partial z}$, and $\frac{\partial v}{\partial z}$, which are averaged within the control volume marked by the dashed box in (a). (g) Evolution of stratification, total vertical shear $\sqrt{(\frac{\partial u}{\partial z})^2 + (\frac{\partial v}{\partial z})^2}$, Richardson number $\frac{N^2}{\sqrt{(\frac{\partial u}{\partial z})^2 + (\frac{\partial v}{\partial z})^2}}$, ϵ , and κ during the enhancement period shaded in (e) and (f). The profiles are made at the center of the control volume.

In the presence of a background current, NIWs can propagate vertically in regions of anti-cyclonic vorticity because of the modification of the effective minimum frequency (Mooers, 1975; Kunze, 1985). To the east of the current core, the vorticity is anti-cyclonic, and hence allows for an eastward and downward propagation pathway of the NIWs. As the NIWs approach and reflect off the eastern slope, not only the vorticity but also the baroclinicity can modify the propagation of the waves, resulting in wave rays with slopes:

$$s_{ray} = s_\rho \pm \sqrt{\frac{\omega^2 - \omega_{min}^2}{N^2}}, \quad (1)$$

where s_ρ is the isopycnal slope, ω is the wave frequency, and $\omega_{min} = f\sqrt{1 + Ro_g - Ri_g^{-1}}$ is the minimum frequency allowable for the waves, $N^2 = \frac{\partial b}{\partial z}$, $Ro_g = \frac{\zeta}{f}$, $Ri_g = \frac{N^2 f^2}{|\nabla_h b|^2}$, b is the buoyancy, and the subscript of h denotes the horizontal gradient (Whitt & Thomas, 2013; Thomas, 2017). According to Eq. (1), the rays of the incident and reflected waves have to be symmetric with respect to isopycnals. As a consequence, the waves are reflected into the deeper strait and propagate westward towards the slantwise critical layer over the western slope.

In the slantwise critical layer, the alignment between the isopycnals and the sloping bottom ensures a background geostrophic flow with $Ro_g = Ri_g^{-1}$, where Ro_g is the Rossby number and Ri_g is the balanced Richardson number (Qu et al., 2021). Consequently, the modifications from the vorticity (encompassed in Ro_g) and the baroclinicity (encompassed in Ri_g) cancel out with each other such that the minimum frequency allowable for NIWs is precisely inertial, $\omega_{min} = f$. According to Eq. (1), $\omega_{min} = f$ ensures $s_{ray} = s_\rho$ for NIWs with $\omega = f$, and hence the associated wave rays are aligned with the sloping bottom in a slantwise critical layer. Moreover, when ω approaches ω_{min} , the group velocity vanishes, leading to wave trapping. So, upon entering the slantwise critical layer, the trapping of the NIWs induce wave amplification and hence enhance the mixing over the western slope of the strait.

4.2 Idealized simulation

A 2.5D idealized simulation is designed to test the conceptual model, in which the ROMS is employed. The domain is based on the realistic bathymetry of the strait at $27^\circ N$ in the across-strait direction and set to be invariant in the along-strait direction. The Coriolis parameter is set to $f = f|_{Lat=27^\circ N}$. The simulation is initialized using the climatological fields at $27^\circ N$ (which are constructed based on the surveys from 2001 to 2019; see Figure S2). The model is forced by an oscillatory wind stress with an amplitude of 0.3 N/m^2 and a frequency of $1.1 f$. See the supporting information for details on the model configuration.

Consistent with the realistic simulation, the idealized simulation also shows that the mixing over the western slope is enhanced with an elevated TKE dissipation rate ϵ and diffusivity κ (Figure 3a and 3b). The pattern of the vertical shear indicates that the NIWs radiate out of the core of the Florida Current, reflect off the eastern slope, and enter the slantwise critical layer over the western slope. The propagation pathway is similar to that in the survey observations and the realistic simulation (Figure 3c and 3d). The averaged ϵ over the western slope exhibits near-inertial pulsing about 3 days after the wind forcing is turned on, which is consistent with the realistic simulation (Figure 3e). The near-inertial pulsing of ϵ is suggestive of a causal link with the NIWs.

Upon entering the slantwise critical layer, the NIWs get trapped, leading to accumulation of wave energy and hence enhanced vertical shear. The idealized simulation shows that the vertical shear in the slantwise critical layer is significantly elevated 2-3 days after the wind forcing is turned on (Figure 3f). Moreover, noting that the background shear is positive (see the early stage in Figure 3f), $\frac{\partial v}{\partial z}$ reaches a maximum when the wave shear aligns with the background shear. As a consequence, this shear alignment phases

240 the mixing enhancement. For instance, the evolution during the mixing enhancement
 241 from 90 to 102 Hr shows that, as the total shear is elevated due to the shear alignment,
 242 the Richardson number is significantly reduced, resulting in the enhanced mixing in the
 243 stratified layer that is evidenced by the elevated ϵ and κ (Figure 3g).

244 In contrast to the coastal slantwise critical layers in the northern Gulf of Mexico
 245 (Qu et al., 2021), the slantwise critical layer in the Straits of Florida is deep, the ver-
 246 tical shear in the background flow is strong, and the NIWs entering the layer are rela-
 247 tively weak with an amplitude one order of magnitude smaller. This leads to a differ-
 248 ence in the mechanisms controlling the near-inertial pulsing of mixing. In the case of the
 249 northern Gulf of Mexico, the strong NIWs significantly modify the background density
 250 field and drive an asymmetric oscillation in the across-shore pressure gradient force with
 251 stronger amplitudes at the phases with onshore currents in the slantwise critical layer
 252 (Qu et al., 2021). Consequently, the convergence of the wave energy flux pulses at cer-
 253 tain phases of the NIWs (i.e., the phases with onshore currents), resulting in a near-inertial
 254 pulsing in the bottom mixing. In the case of the Straits of Florida, the NIWs are in a
 255 weak and linear regime, and the near-inertial pulsing of mixing is driven by the shear
 256 alignment that occurs near-inertially. Nevertheless, both mixing enhancements are due
 257 to wave trapping in the slantwise critical layers.

258 5 Discussion

259 Sixty tropical storms/hurricanes passed the Straits of Florida from 2001 to 2020
 260 (see Figure 4a for the storm tracks), indicating a significant amount of energy input into
 261 the NIW field. However, NIWs form not only during tropical storms/hurricanes but also
 262 in other strong-wind events that are not induced by tropical storms/hurricanes. Con-
 263 sequently, enhancement of mixing in the deep strait can be also driven during the non-
 264 storm wind events via NIW trapping. Here, we discuss the relative importance of trop-
 265 ical storms/hurricanes in generating NIWs in the Straits versus other strong-wind events.
 266 The wind events over the Straits are recognized if the wind speed is over 10 m/s and are
 267 classified as either storm events or strong-wind events depending on whether a storm passed
 268 by the strait. Figure 4d and 4e show the statistics of these two groups of wind events
 269 in terms of strength and persistence. The storm events tend to occur in summer and fall,
 270 exhibiting short and intermittent characteristics combined with strong bursts, while the
 271 strong-wind events often occur in winter, exhibiting long and regulated persistence with
 272 mildly strong winds.

273 To understand the relative importance of these two groups of winds on energizing
 274 NIWs, the wind work of each group is estimated via a slab mixed layer model as follows:

$$275 \frac{\partial u_{ML}}{\partial t} - fv_{ML} = \frac{\tau_x}{\rho_0 H_{ML}} - ru_{ML}, \quad (2)$$

$$276 \frac{\partial v_{ML}}{\partial t} + fu_{ML} = \frac{\tau_y}{\rho_0 H_{ML}} - rv_{ML}, \quad (3)$$

278 where (u_{ML}, v_{ML}) are the mixed layer velocities, $f = f|_{27^\circ N}$ is the Coriolis parame-
 279 ter, (τ_x, τ_y) is the wind stress, $\rho_0 = 1025 \text{ kg/m}^3$ is the reference density, $H_{ML} = 50 \text{ m}$
 280 is the mixed layer thickness, and $r = \frac{1}{2}f$ is the damping coefficient (Pollard & Millard Jr,
 281 1970). The solutions of the slab mixed layer model are not sensitive to the magnitude
 282 of r and do not qualitatively change if the coefficient is in the range $1/r = 0.1\text{--}1 \text{ days}$
 283 (D'Asaro, 1985; Whitt & Thomas, 2015). The wind stress is calculated based on a quadratic
 284 equation, $\vec{\tau} = C_d \rho_{air} |\vec{U}_{10}| \vec{U}_{10}$, where $C_d = 1.5 \times 10^{-3}$ is the drag coefficient, $\rho_{air} =$
 285 1.225 kg/m^3 is the air density, and \vec{U}_{10} is the wind velocity 10 m above the sea (Cushman-
 286 Roisin & Beckers, 2011). The wind velocity is extracted from the CFSR/NOAA dataset
 287 and averaged between $-80^\circ W$ and $-79^\circ W$ and along $27^\circ N$.

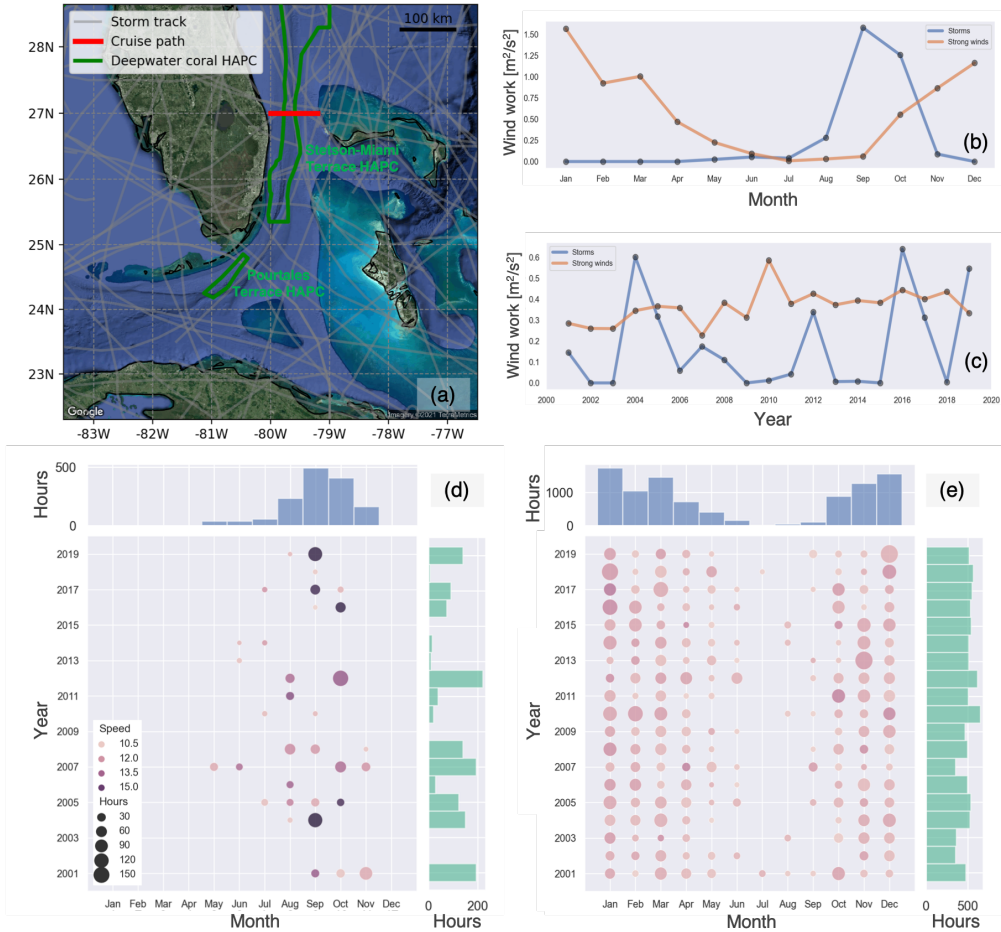


Figure 4. (a) The Storm tracks (gray lines) from 2001 to 2020 and the deep-water coral habitat areas of particular concern (HAPCs; green polygons). The storm tracks are from IBTrACS. (b and c) Wind work $WORK_{TS}$ (blue) and $WORK_{SW}$ (yellow) as functions of month and year. (d) Scatter plot of the wind events related to the tropical storms/hurricanes from 2001 to 2009. The color denotes the wind speed in units of m/s, and the size denotes the duration in units of hours. Histograms of the duration are attached at the axes. (e) Same as (d) but for the non-storm wind events. The winds are averaged between $-80^{\circ}W$ and $-79^{\circ}W$ and along $27^{\circ}N$ using the CFSR dataset.

Forced by the wind stress, the slab mixed layer model is integrated to yield the mixed layer velocities so that the wind work can be estimated. By definition, the wind work integrated through a certain period T follows

$$WORK = \int_T \frac{\tau_x u_{ML} + \tau_y v_{ML}}{\rho_0 H_{ML}} dt . \quad (4)$$

The wind work represents the energy input into the NIW field by the winds and yields an upper bound on the wave energy flux into the ocean interior. The wind work is attributed to the two groups by integrating through two different periods. The period for the tropical storms/hurricanes T_{TS} is defined by when the wind speed is over 10 m/s and a storm passes over, while the period for the strong-wind events T_{SW} is when the wind speed surpasses the same cutoff but the high speed is not driven by any tropical storms/hurricanes. The wind work $WORK_{TS}$ and $WORK_{SW}$ are then determined by integrating over T_{TS} and T_{SW} , respectively. The statistics show $WORK_{TS}$ and $WORK_{SW}$ as functions of month and year (Figure 4b and 4b). If shown in month (year), the wind work is calculated by integrating Eq. (4) over the T_{TS}/T_{SW} of a certain month (year) over all years (months). It is suggested that $WORK_{TS}$ and $WORK_{SW}$ take turns to dominate in different seasons with similar magnitudes, and $WORK_{SW}$ maintains at a stable level with the magnitude comparable to $WORK_{TS}$ of the years with intense storms. Consequently, it could be inferred that the long persistence of the winds makes the strong-wind events an equivalently important contributor to energize the NIWs. Overall, both the tropical storms/hurricanes and strong-wind events input a significant amount of energy into the NIW field and could play equally important roles on driving the enhancement of bottom-mixing, yielding potential environmental implications in the deep strait.

The Straits of Florida is a habitat with extensive deep-sea coral ecosystems (Reed et al., 2013). Deep-sea corals provide shelters and host deep-water ecosystems (Wilson et al., 2006). Two deep-water coral habitat areas of particular concern (HAPCs; Figure 4a) are designated between Florida and the Bahamas in the deep western strait (NOAA, 2010), where the mixing could be enhanced by NIWs. The mixing enhancement could alter the levels of temperature, oxygen, and PH that the corals experience and may cause sediment resuspension that would provide particulate organic matter for the corals, suggesting important implications for the benthic ecosystems.

Another potential impact of the enhanced mixing worth noting is related to Antarctic Intermediate Water (AAIW). Induced by the upslope bottom Ekman transport, AAIW blankets over the western bottom of the strait (Seim et al., 1999). AAIW is a cold, low salinity water mass that distinguishes from the upper warmer, saltier water in the strait which is originated from the subtropical South Atlantic (Atkinson, 1983; Schmitz Jr & Richardson, 1991). The enhanced mixing by NIWs could affect the abyssal diapycnal transport and hence potentially modify the properties of AAIW before it joins the North Atlantic, which could have significant implications for the distribution of biogeochemical tracers downstream.

Acknowledgments

This work was funded by the SUNRISE project, NSF grant numbers OCE-1851450 (L.Q. and L.N.T). J.G. gratefully acknowledges support from the French National Agency for Research (ANR) through the project DEEPER (ANR19CE01000201). The research cruises used in this study were funded by the Western Boundary Time Series project, which is supported by the Climate Program Office of the NOAA. The CTD and ADCP data used in this study are available online (<https://www.aoml.noaa.gov/phod/wbts/data.php>). The satellite imageries from the MODIS-AQUA are available online through the WORLDVIEW supported by the National Aeronautics and Space Administration (<https://worldview.earthdata.nasa.gov>). We acknowledge PRACE and GENCI for awarding us access to HPC resources Joliot-Curie Rome and SKL from GENCI-TGCC (Grants 2020-A0090112051, 2019gch0401 and PRACE project 2018194735) and HPC facilities DATARMOR of Ple de Calcul Intensif pour la Mer at Ifremer Brest France. We thank Gildas Cambon and Sbastien Theetthen for their contribution in the development of the realistic numerical simulation GIGATL1. The information about the GIGATL1 can be found at (<https://doi.org/10.5281/zenodo.4948523>). We thank Jennifer MacKinnon and Kathryn Shamberger for very helpful suggestions when preparing this manuscript.

344 **References**

- 345 Alford, M. H., MacKinnon, J. A., Simmons, H. L., & Nash, J. D. (2016). Near-
 346 inertial internal gravity waves in the ocean. *Annual review of marine science*,
 347 8, 95–123.
- 348 Asselin, O., & Young, W. R. (2020). Penetration of wind-generated near-inertial
 349 waves into a turbulent ocean. *Journal of Physical Oceanography*, 50(6), 1699–
 350 1716.
- 351 Atkinson, L. P. (1983). Distribution of antarctic intermediate water over the blake
 352 plateau. *Journal of Geophysical Research: Oceans*, 88(C8), 4699–4704.
- 353 Becker, J. J., Sandwell, D. T., Smith, W. H. F., Braud, J., Binder, B., Depner, J.,
 354 ... Weatherall, P. (2009, November). Global Bathymetry and Elevation Data
 355 at 30 Arc Seconds Resolution: SRTM30_PLUS. *Mar. Geod.*, 32(4), 355–371.
 356 doi: 10.1080/01490410903297766
- 357 Cacchione, D., Pratson, L., & Ogston, A. (2002). The shaping of continental slopes
 358 by internal tides. *Science*, 296, 724-727.
- 359 Cacchione, D., & Wunsch, C. (1974). Experimental study of internal waves over a
 360 slope. *Journal of Fluid Mechanics*, 66, 223-239.
- 361 Callies, J., & Ferrari, R. (2018). Dynamics of an abyssal circulation driven by
 362 bottom-intensified mixing on slopes. *Journal of Physical Oceanography*, 48,
 363 1257-1282.
- 364 Canuto, V. M., Howard, A., Cheng, Y., & Dubovikov, M. (2001). Ocean turbulence.
 365 part i: One-point closure modelmomentum and heat vertical diffusivities. *Jour-
 366 nal of Physical Oceanography*, 31(6), 1413–1426.
- 367 Carton, J., & Giese, B. (2008). A reanalysis of ocean climate using Simple Ocean
 368 Data Assimilation (SODA). *Mon. Weath. Rev.*, 136, 2999-3017.
- 369 Chalamalla, V., Gayen, B., Scotti, A., & Sarkar, S. (2013). Turbulence during the
 370 reflection of internal gravity waves at critical and near-critical slopes. *Journal*
 371 *of Fluid Mechanics*, 729, 47-68.
- 372 Cushman-Roisin, B., & Beckers, J.-M. (2011). *Introduction to geophysical fluid dy-
 373 namics: physical and numerical aspects*. Academic press.
- 374 D'Asaro, E. A. (1985). The energy flux from the wind to near-inertial motions in the
 375 surface mixed layer. *Journal of Physical Oceanography*, 15(8), 1043–1059.
- 376 Ferrari, R., Mashayek, A., McDougall, T., Nikurashin, M., & Campin, J. (2016).
 377 Turning ocean mixing upside down. *Journal of Physical Oceanography*, 46,
 378 2239-2261.
- 379 Garcia, R. F., & Meinen, C. S. (2014). Accuracy of florida current volume transport
 380 measurements at 27 n using multiple observational techniques. *Journal of At-
 381 mospheric and Oceanic Technology*, 31(5), 1169–1180.
- 382 Gregg, M. (1989). Scaling turbulent dissipation in the thermocline. *Journal of Geo-
 383 physical Research: Oceans*, 94(C7), 9686–9698.
- 384 Gregg, M., Alford, M., Kontoyiannis, H., Zervakis, V., & Winkel, D. (2012). Mixing
 385 over the steep side of the cycladic plateau in the aegean sea. *Journal of Marine*
 386 *Systems*, 89(1), 30–47.
- 387 Gregg, M., Winkel, D., MacKinnon, J., & Lien, R. (1999). Mixing over shelves
 388 and slopes. In *Mu®ller, p., henderson, d.(eds.), dynamics of oceanic internal*
 389 *gravity waves ii, proceedings, hawaiian winter workshop* (pp. 35–42).
- 390 Knapp, K. R., Kruk, M. C., Levinson, D. H., Diamond, H. J., & Neumann, C. J.
 391 (2010). The international best track archive for climate stewardship (ibtracs)
 392 unifying tropical cyclone data. *Bulletin of the American Meteorological Society*,
 393 91(3), 363–376.
- 394 Kunze, E. (1985). Near-inertial wave propagation in geostrophic shear. *Journal of*
 395 *Physical Oceanography*, 15(5), 544–565.
- 396 Kunze, E., & Llewellyn Smith, S. (2004). The role of small-scale topography in tur-
 397 bulent mixing of the global ocean. *Oceanography*, 17, 55-64.

- 398 Kunze, E., & Smith, S. L. (2004). The role of small-scale topography in turbulent
 399 mixing of the global ocean. *Oceanography*, 17(1), 55–64.
- 400 McDougall, T., & Ferrari, R. (2017). Abyssal upwelling and downwelling driven by
 401 near-boundary mixing. *Journal of Physical Oceanography*, 47, 261–283.
- 402 Meinen, C. S., Baringer, M. O., & Garcia, R. F. (2010). Florida current transport
 403 variability: An analysis of annual and longer-period signals. *Deep Sea Research
 404 Part I: Oceanographic Research Papers*, 57(7), 835–846.
- 405 Mooers, C. N. (1975). Several effects of a baroclinic current on the cross-stream
 406 propagation of inertial-internal waves. *Geophysical and Astrophysical Fluid Dy-
 407 namics*, 6(3), 245–275.
- 408 Moum, J., Caldwell, D., Nash, J., & Gunderson, G. (2002). Observations of bound-
 409 ary mixing over the continental slope. *Journal of Physical Oceanography*,
 410 32(7), 2113–2130.
- 411 Nash, J., Alford, M., Kunze, E., Martini, K., & Kelly, S. (2007). Hotspots of deep
 412 ocean mixing on the oregon continental slope. *Geophysical Research Letters*,
 413 34(1).
- 414 NOAA. (2010). Fisheries of the caribbean, gulf of mexico, and south atlantic; com-
 415 prehensive ecosystem- based amendment for the south atlantic region. *Federal
 416 Register*, 75(119), 35330–35335.
- 417 Pollard, R. T., & Millard Jr, R. (1970). Comparison between observed and sim-
 418 ultated wind-generated inertial oscillations. In *Deep sea research and oceano-
 419 graphic abstracts* (Vol. 17, pp. 813–821).
- 420 Polzin, K. L., Toole, J. M., & Schmitt, R. W. (1995). Finescale parameterizations of
 421 turbulent dissipation. *Journal of physical oceanography*, 25(3), 306–328.
- 422 Qu, L., Thomas, L. N., & Hetland, R. D. (2021). Near-inertial wave critical layers
 423 over sloping bathymetry. *Journal of Physical Oceanography*.
- 424 Reed, J. K., Messing, C., Walker, B. K., Brooke, S., Correa, T. B., Brouwer, M., ...
 425 Farrington, S. (2013). Habitat characterization, distribution, and areal extent
 426 of deep-sea coral ecosystems off florida, southeastern usa. *Caribbean journal of
 427 science*, 47(1), 13–30.
- 428 Saha, S., Moorthi, S., Pan, H.-L., Wu, X., Wang, J., Nadiga, S., ... others (2010).
 429 The ncep climate forecast system reanalysis. *Bulletin of the American Meteo-
 430 rological Society*, 91(8), 1015–1058.
- 431 Schmitz Jr, W. J., & Richardson, P. L. (1991). On the sources of the florida current.
 432 *Deep Sea Research Part A: Oceanographic Research Papers*, 38, S379–S409.
- 433 Seim, H. E., Winkel, D. P., Gawarkiewicz, G., & Gregg, M. C. (1999). A benthic
 434 front in the straits of florida and its relationship to the structure of the florida
 435 current. *Journal of physical oceanography*, 29(12), 3125–3132.
- 436 Shchepetkin, A. F., & McWilliams, J. C. (2005). The regional oceanic modeling
 437 system (roms): a split-explicit, free-surface, topography-following-coordinate
 438 oceanic model. *Ocean Modelling*, 9(4), 347–404.
- 439 Szuts, Z. B., & Meinen, C. (2013). Salinity transport in the florida straits. *Journal
 440 of Atmospheric and Oceanic Technology*, 30(5), 971–983.
- 441 Thomas, L. N. (2017). On the modifications of near-inertial waves at fronts: implica-
 442 tions for energy transfer across scales. *Ocean Dynamics*, 67(10), 1335–1350.
- 443 Umlauf, L., & Burchard, H. (2003). A generic length-scale equation for geophysical
 444 turbulence models. *Journal of Marine Research*, 61(2), 235–265.
- 445 Warner, J. C., Sherwood, C. R., Arango, H. G., & Signell, R. P. (2005). Perfor-
 446 mance of four turbulence closure models implemented using a generic length
 447 scale method. *Ocean Modelling*, 8(1-2), 81–113.
- 448 Whitt, D. B., & Thomas, L. N. (2013). Near-inertial waves in strongly baroclinic
 449 currents. *Journal of Physical Oceanography*, 43(4), 706–725.
- 450 Whitt, D. B., & Thomas, L. N. (2015). Resonant generation and energetics of wind-
 451 forced near-inertial motions in a geostrophic flow. *Journal of Physical Oceanog-
 452 raphy*, 45(1), 181–208.

- 453 Wilson, S. K., Graham, N. A., Pratchett, M. S., Jones, G. P., & Polunin, N. V.
454 (2006). Multiple disturbances and the global degradation of coral reefs: are
455 reef fishes at risk or resilient? *Global Change Biology*, 12(11), 2220–2234.
- 456 Winkel, D. P., Gregg, M. C., & Sanford, T. B. (2002). Patterns of shear and tur-
457 bulence across the florida current. *Journal of physical oceanography*, 32(11),
458 3269–3285.
- 459 Wunsch, C., & Ferrari, R. (2004). Vertical mixing, energy, and the general circula-
460 tion of the oceans. *Annu. Rev. Fluid Mech.*, 36, 281–314.
- 461 Young, W., & Jelloul, M. B. (1997). Propagation of near-inertial oscillations through
462 a geostrophic flow. *Journal of marine research*, 55(4), 735–766.

Accepted Article